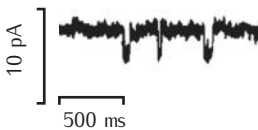


# Models of active ion channels

There are many types of active ion channel beyond the squid giant axon sodium and potassium voltage-gated ion channels studied in Chapter 3, including channels gated by ligands such as calcium. The aim of this chapter is to present methods for modelling the kinetics of voltage-gated and ligand-gated ion channels at a level suitable for inclusion in compartmental models. The chapter will show how the basic formulation used by Hodgkin and Huxley of independent gating particles can be extended to describe many types of ion channel. This formulation is the foundation for **thermodynamic models**, which provide functional forms for the rate coefficients derived from basic physical principles. To improve on the fits to data offered by models with independent gating particles, the more flexible **Markov models** are introduced. When and how to interpret kinetic schemes probabilistically to model the stochastic behaviour of single ion channels will be considered. Experimental techniques for characterising channels are outlined and an overview of the biophysics of channels relevant to modelling channels is given.



**Fig. 5.1** Single channel recording of the current passing through an acetylcholine-activated channel recorded from frog muscle in the presence of acetylcholine (Neher and Sakmann, 1976). Though there is some noise, the current can be seen to flip between two different levels. Reprinted by permission from Macmillan Publishers Ltd: *Nature* 260, 779–802, © 1976.

Over 100 types of ion channel are known. Each type of channel has a distinct response to the membrane potential, intracellular ligands, such as calcium, and extracellular ligands, such as neurotransmitters. The membrane of a single neuron may contain a dozen or more different types, with the density of each type depending on its location in the membrane. The distribution of ion channels over a neuron affects many aspects of neuronal function, including the shape of the action potential, the duration of the refractory period, how synaptic inputs are integrated and the influx of calcium into the cell. When channels are malformed due to genetic mutations, diseases such as epilepsy, chronic pain, migraine and deafness can result (Jentsch, 2000; Catterall *et al.*, 2008).

Models of neurons containing multiple channel types are an invaluable aid to understanding how combinations of ion channels can affect the time course of the membrane potential. For example, later on in this chapter, it will be shown that the addition of just one type of channel to a Hodgkin–Huxley (HH) model neuron can have profound effects on its firing properties, effects that could not be predicted by verbal reasoning alone.

In order to build neuron models with multiple channel types, models of individual constituent channel types must be constructed. In Chapter 3 it was shown how voltage clamp currents of squid giant axon sodium and potassium channels could be reproduced approximately by a model in which the channel opening and closing is controlled by a set of independent gating particles. In this chapter, it will be shown how this method can be extended to different types of voltage- and ligand-gated channels.

Independent gating particle models are sufficiently accurate to explore many questions about neuronal electrical activity but, even with optimal parameter tuning, there are discrepancies between their behaviour and the behaviour of certain types of channel. An improved fit to the data can be achieved by using Markov models, which are not constrained by the idea of independent gating particles and consider the state of the entire channel, rather than constituent gating particles.

A further modification to channel models is required in order to explain voltage clamp recordings from single channels made using the patch clamp technique, pioneered by Neher and Sakmann (1976). Rather than being smoothly varying, single channel currents switch randomly between zero and a fixed amplitude (Figure 5.1). This chapter will show how probabilistic Markov models can be used to understand single channel data and will introduce a method for simulating a single channel stochastically. It will also consider under what circumstances this type of simulation is necessary.

The principal thrust of this chapter is how to construct models of the dependence of ion channel conductance on the membrane potential and concentrations of intracellular ligands. The chapter will also touch on the considerable understanding of the structure and function of ion channels at the level of the movement of molecules within channel proteins, which has culminated in the derivation of the 3D structure of ion channels (Figure 5.2) from X-ray crystallography (Doyle *et al.*, 1998). While much of this understanding is more detailed than needed for modelling the electrical behaviour of neurons, modelling studies can be informed by the concepts of ion channel structure and function. In this chapter, the theory of chemical reaction rates is applied to channel gating to produce thermodynamic models of channels, which naturally incorporate temperature and voltage dependence. Incorporating physical theory into channel models is desirable as it is likely to make them more accurate. A basic understanding of ion channel structure and function is also important when interpreting the data on which channel models are based.

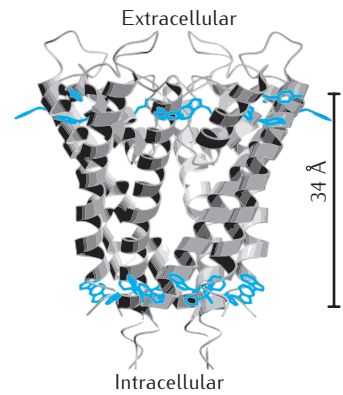


**Fig. 5.2** Structure of a potassium channel (the KcsA channel) from the soil bacterium *Streptomyces lividans*, determined by X-ray crystallography by Doyle *et al.* (1998). The *kcsA* gene was identified, expressed and characterised electrophysiologically by Schrempf *et al.* (1995). The KcsA channel is blocked by caesium ions, giving rise to its name. From Doyle *et al.* (1998). Reprinted with permission from AAAS.

## 5.1 Ion channel structure and function

A vast range of biochemical, biophysical and molecular biological techniques have contributed to the huge gain in knowledge of channel structure and function since Hodgkin and Huxley's seminal work. This section provides a very brief outline of our current understanding; Hille (2001) and more recent review papers such as Tombola *et al.* (2006) provide a comprehensive account.

### Box 5.1 | The IUPHAR scheme for naming channels

The International Union of Pharmacology (IUPHAR) has formalised a naming system for ion channel proteins in the voltage-gated-like superfamily based on both structural protein motifs and primary functional characteristics (Yu *et al.*, 2005).

Under this scheme, channels are organised and named based on prominent functional characteristics and structural relationships. Where there is a principal permeating ion, the name begins with the chemical symbol of the ion. This is followed by the principal physiological regulator or classifier, often written as a subscript. For example, if voltage is the principal regulator of the channel, the subscript is 'v', as in  $\text{Na}_v$  or  $\text{Ca}_v$ . Where calcium concentration is the principal channel regulator the subscript is 'Ca', as in  $\text{K}_{\text{Ca}}$ . Examples of other structural classifications are the potassium channel families  $\text{K}_{\text{ir}}$  and  $\text{K}_{2\text{P}}$ . Two numbers separated by a dot follow the subscript, the first representing gene subfamily and the second the specific channel isoform (e.g.  $\text{K}_v3.1$ ).

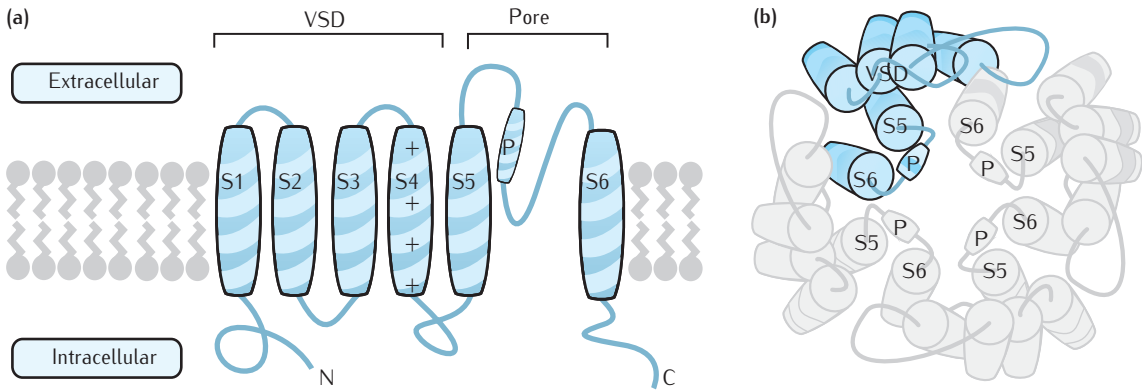
Where there is no principal permeating ion in a channel family, the family can be identified by the gating regulator or classifier alone. Examples are the cyclic-nucleotide-gated channel family (CNG), the hyperpolarisation-activated cyclic-nucleotide-gated channel family (HCN), the transient receptor potential channel family (TRP) and the two-pore-channels family (TPC).

In the HH model, there are four independent gating particles for the potassium conductance. This happens to correspond to the four subunits of the tetrameric, delayed rectifier potassium channel. However, this type of correspondence is not true of all independent gating particles models. For example, in the HH model of the sodium channel there are three activating particles, but the sodium channel has one principal subunit that contains four sets of voltage-sensitive domains and pore-forming domains.

Each ion channel is constructed from one or more protein subunits. Those that form the pore within the membrane are called **principal subunits**. There may be one principal subunit (e.g. in  $\text{Na}^+$  and  $\text{Ca}^{2+}$  channels), or more than one (e.g. in voltage-gated  $\text{K}^+$  channels). Ion channels with more than one principal subunit are called **multimers**; if the subunits are all identical, they are **homomers**, and if not, they are **heteromers**. Multimeric channel structures were presaged by Hodgkin and Huxley's idea (Chapter 3) of channels as gates containing multiple gating particles. However, there is not generally a direct correspondence between the model gating particles and channel subunits. As the number of known channel proteins has increased, systematic naming schemes for them, such as the IUPHAR naming scheme (Box 5.1), have been developed.

An ion channel may also have **auxiliary subunits** attached to the principal subunits or to other auxiliary subunits. The auxiliary subunits may be in the membrane or the cytoplasm and can modulate, or even change drastically, the function of the primary subunits. For example, when the  $\text{K}_v1.5$  type of principal subunit is expressed in oocytes alone (Section 5.3.3) or with the  $\text{K}_v\beta2$  auxiliary subunit, the resulting channels are non-inactivating. However, when expressed with the  $\text{K}_v\beta1$  subunit the channels are inactivating (Heinemann *et al.*, 1996).

The secondary structure of one of the four principal subunits of a voltage-gated potassium channel is shown in Figure 5.3a. The polypeptide chain is arranged into segments organised into  $\alpha$ -helices and connecting



loops. Figure 5.3b shows the 3D arrangement of the four principal subunits in a closed conformation of the channel protein. The S5 and S6 segments form the lining of the pore, and the S1–S4 segments form a voltage-sensitive domain (VSD). The 3D structure of a number of channels has been elucidated, including the weakly voltage-gated KcsA potassium channel shown in Figure 5.2 (Doyle *et al.*, 1998), a potassium channel from the bacterium *Aeropyrum pernix* (Jiang *et al.*, 2003) and the eukaryotic *Shaker* K<sub>v</sub>1.2 voltage-gated potassium channel (Long *et al.*, 2005).

As seen in Chapter 3, Hodgkin and Huxley proposed a voltage-sensing mechanism consisting of the movement of charged particles within the membrane. Such a mechanism has been broadly confirmed in the S4 segment of the voltage-gated potassium channel VSD. A number of positively charged residuals within the S4 segment (called **gating charges**) experience the electric force due to the membrane potential. The resultant movements of the gating charges lead to other segments in the channel moving. The precise nature of the movement is currently not known, and may depend on the type of channel. This shift leads to a change in the pore conformation through an interaction of the S4–S5 link with the *neighbouring* subunit's S6 segment. It is hypothesised that a hinge in the S6 helical segment forms the basis of the gate, allowing ions to flow in the open state, and limiting flow in the closed state. Evidence for this comes both from mutations in the S6 helical segment and data from X-ray crystallography (Tombola *et al.*, 2006).

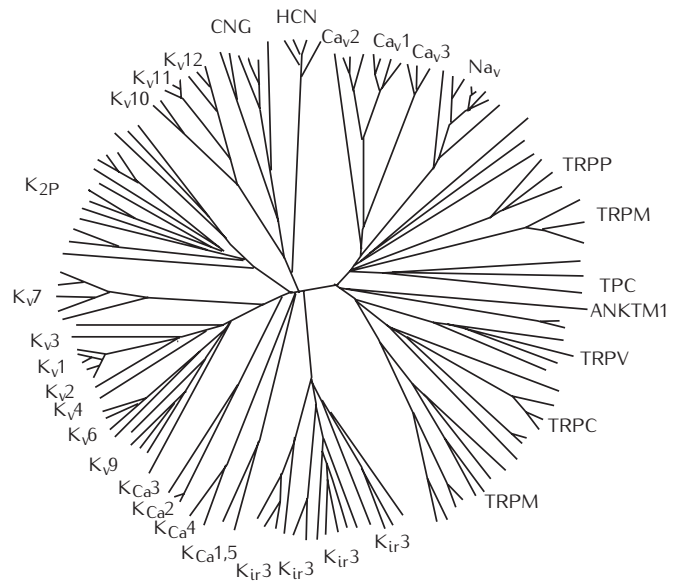
The changes in conformation of channel proteins over periods of nanoseconds during gating and permeation of ions through the pore can be modelled using molecular dynamics simulations at an atomic level (see Roux *et al.* (2004) for a review). This type of model is much more detailed than is needed to understand how the distribution of different channel types throughout the cellular membrane leads to the electrical activity characteristic of different neurons.

**Fig. 5.3** (a) Secondary structure of one subunit of a voltage-gated potassium channel (based on Tombola *et al.*, 2006). A number of segments of the polypeptide chain are arranged to form  $\alpha$ -helices, which are connected together by loops. Six of these  $\alpha$ -helices span the membrane and are labelled S1–S6, and there is also a P  $\alpha$ -helix, in the loop that joins the S5 and S6 transmembrane segments. The S4 segment contains a number of charged residues and, along with segments S1–S3, makes up the voltage-sensing domain (VSD) of the subunit. Segments S5, S6 and P make up the pore region. Both the N-terminal and C-terminal of the polypeptide project into the cytoplasm. (b) The tertiary structure of the principal subunits in a closed conformation of the channel viewed from above. The four subunits (one of which is highlighted) can be seen to form a central pore, lined by the S5, S6 and P segments of each subunit.

## 5.2 Ion channel nomenclature

In the early 1980s the genes of ion channels began to be sequenced. With the completion of the human genome, genes for over 140 channels have been

**Fig. 5.4** The superfamily of mammalian voltage-gated-like ion channels, organised as a phylogenetic tree constructed from the similarities between the amino acid sequences of the pore regions of the channels. There are 143 members of the superfamily, organised into a number of family groups:  $\text{Na}_v$ ,  $\text{Ca}_v$ ,  $\text{K}_v$ ,  $\text{K}_{\text{Ca}}$ , CNG/HCN,  $\text{K}_{2\text{P}}$ / $\text{K}_{\text{ir}}$ , TRP and TPC. Although the  $\text{K}_{\text{Ca}2}$  and  $\text{K}_{\text{Ca}3}$  subfamilies are purely ligand-gated, because of the structural similarity of the pore, they still belong to the voltage-gated superfamily. Adapted from Yu *et al.* (2005), with permission from the American Society for Pharmacology and Experimental Therapeutics.



discovered. Each channel gene is named according to the scheme used for the organism in which it occurs. The prefix of the gene gives some information about the type of channel to which it refers; for example, genes beginning with KCN are for potassium channels. This **gene nomenclature** is set by organism-specific committees; for example, The Human Genome Organisation Gene Nomenclature Committee is responsible for the naming of human genes.

Family trees of ion channels can be made by grouping the amino acid sequences corresponding to each gene (Figure 5.4). Within each family, channels with the same principal permeant ion are grouped together, and there are subgroups of channels which are voltage-gated or ligand-gated. The phylogenetic tree also reflects the similarities in the channel structures such as the number of transmembrane segments.

This structure is reflected in the system of naming cation channels adopted by the IUPHAR, sometimes referred to as the **clone nomenclature** (Hille, 2001). The scheme incorporates the ion selectivity and the principal activator, as well as the degree of sequence similarity (Box 5.1). Because of its functional relevance, the IUPHAR scheme is in common use among biophysicists and increasingly by electrophysiologists. The gene nomenclature does not reflect as much of the function and structure as the IUPHAR scheme, particularly in the case of potassium channels (Gutman *et al.*, 2005). Nevertheless, even the IUPHAR scheme has quirks, such as including in the calcium-activated potassium family,  $\text{K}_{\text{Ca}5.1}$ , a type of potassium channel whose gating is dependent on intracellular  $\text{Na}^+$  and  $\text{Cl}^-$  but not  $\text{Ca}^{2+}$ .

A number of gene families of ion channels, excluding channels activated by extracellular ligands such as synaptic channels, are shown in Table 5.1. Apart from the chloride channels, all the families belong to the superfamily of voltage-gated-like channels, which has at least 143 members (Yu *et al.*, 2005). The superfamily is called voltage-gated-like because while most of

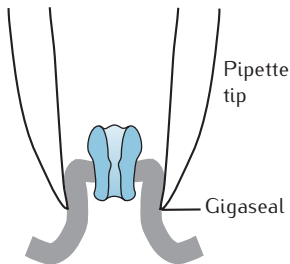


**Fig. 5.5** The patch clamp technique. A fire-polished glass electrode with a tip of less than  $5\ \mu\text{m}$  in diameter has been placed on the surface of a cell and suction has been applied so that a very tight gigaseal has been formed between the electrode and the membrane surrounding a single channel. The electrode has then been withdrawn from the cell membrane, ripping the small patch of membrane away from the cell, to form an 'inside-out' patch.

**Table 5.1** Families of channel genes and their corresponding proteins

Human gene prefix	IUPHAR protein prefix	Ion selectivity	Activators
SCN	Na <sub>v</sub>	Na <sup>+</sup>	V↑
CACN	Ca <sub>v</sub>	Ca <sup>2+</sup>	V↑
KCN	K <sub>v</sub>	K <sup>+</sup>	V↑
KCNA	K <sub>v1</sub>	K <sup>+</sup>	V↑
KCNB	K <sub>v2</sub>	K <sup>+</sup>	V↑
KCNC	K <sub>v3</sub>	K <sup>+</sup>	V↑
KCND	K <sub>v4</sub>	K <sup>+</sup>	V↑
KCNQ	K <sub>v7</sub>	K <sup>+</sup>	V↑
KCNMA	K <sub>Ca1</sub>	K <sup>+</sup>	Ca <sup>2+</sup> , V↑
KCNN	K <sub>Ca2</sub>	K <sup>+</sup>	Ca <sup>2+</sup> ↑
KCNJ	K <sub>ir</sub>	K <sup>+</sup>	G-proteins, V↑
KCNK	K <sub>2P</sub>	K <sup>+</sup>	Leak, various modulators
HCN	HCN	K <sup>+</sup> , Na <sup>+</sup>	V↓
CNG	CNG	Ca <sup>2+</sup> , K <sup>+</sup> , Na <sup>+</sup>	cAMP, cGMP
TRP	TRP	Ca <sup>2+</sup> , Na <sup>+</sup>	Heat, second messengers
CLCN	–	Cl <sup>–</sup>	V↓, pH
CLCA	–	Cl <sup>–</sup>	Ca <sup>2+</sup>

Data from IUPHAR *Compendium of Voltage-Gated Ion Channels* (Catterall *et al.*, 2005a, b; Gutman *et al.*, 2005; Wei *et al.*, 2005; Kubo *et al.*, 2005; Goldstein *et al.*, 2005; Hofmann *et al.*, 2005; Clapham *et al.*, 2005; Jentsch *et al.*, 2005).

its channels are voltage-gated, some are gated by intracellular ligands, second messengers or stimuli such as heat. For example, CNG channels, activated by the cyclic nucleotides cAMP (cyclic adenosine monophosphate) and cGMP (cyclic guanosine monophosphate), are expressed in rod and cone photoreceptor neurons and the cilia of olfactory neurons (Hofmann *et al.*, 2005). Similarly, members of the TRP family are involved in heat or chemical sensing.

Heterologous expression of the cloned DNA of a channel (Section 5.3.3) allows the physiological characteristics of channel proteins to be determined. The currents recorded under voltage clamp conditions can be matched to the existing gamut of currents which have been measured using other techniques such as channel blocking, and given ad hoc names such as the A-type current  $I_A$  or the T-type current  $I_{CaT}$ . This **ad hoc nomenclature** for channels is sometimes still used when the combination of genes expressed in a preparation is not known. However, as use of the IUPHAR system by neurophysiologists and modellers becomes more prevalent (see, for example, Maurice *et al.*, 2004), terms such as ‘Ca<sub>v</sub>3.1-like’ (instead of  $I_{CaT}$ ) are also now used when the presence of a particular channel protein is not known. The currents that are associated with some well-known voltage- and ligand-gated channel proteins are shown in Table 5.2.

The presence of the gene which encodes a particular channel protein, as opposed to current, can be determined using knockout studies (Stocker,

**Table 5.2** Summary of important currents, their corresponding channel types and sample parameters.

Current	Channel proteins	Other names	Activation			Inactivation			Note
			$V_{1/2}$ (mV)	$\sigma$ (mV)	$\tau$ (ms)	$V_{1/2}$ (mV)	$\sigma$ (mV)	$\tau$ (ms)	
$I_{Na}$	$Na_v1.1-1.3, 1.6$		-30	6	0.2	-67	-7	5	a
$I_{NaP}$	$Na_v1.1-1.3, 1.6$		-52	5	0.2	-49	-10	1500	b
$I_{CaL}$	$Ca_v1.1-1.4$	HVA <sub>l</sub>	9	6	0.5	4	2	400	c
$I_{CaN}$	$Ca_v2.2$	HVA <sub>m</sub>	-15	9	0.5	-13	-19	100	d
$I_{CaR}$	$Ca_v2.3$	HVA <sub>m</sub>	3	8	0.5	-39	-9	20	e
$I_{CaT}$	$Ca_v3.1-3.3$	LVA	-32	7	0.5	-70	-7	10	f
$I_{PO}$	$K_v3.1$	Fast rectifier	-5	9	10	—	—	—	g
$I_{DR}$	$K_v2.2, K_v3.2...$	Delayed rectifier	-5	14	2	-68	-27	90	h
$I_A$	$K_v1.4, 3.4, 4.1, 4.2...$		-1	15	0.2	-56	-8	5	i
$I_M$	$K_v7.1-7.5$	Muscarinic	-45	4	8	—	—	—	j
$I_D$	$K_v1.1-1.2$		-63	9	1	-87	-8	500	k
$I_h$	HCN1-4	Hyperpolarisation-activated	-75	-6	1000	—	—	—	l
$I_C$	$K_{Ca}1.1$	BK, maxi-K(Ca), fAHP	V & Ca <sup>2+</sup> -dep			—	—	—	m
$I_{AHP}$	$K_{Ca}2.1-2.3$	SK1-3, mAHP	0.7 $\mu$ M		40	—	—	—	n
$I_{sAHP}$	$K_{Ca}?$	Slow AHP	0.08 $\mu$ M		200	—	—	—	o

Parameters are for voltage-dependent activation and inactivation in one model of a channel; other models have significantly different parameters.  $K_{0.5}$  (Section 5.6) is given for calcium dependent K<sup>+</sup> channels. Time constants are adjusted to 37°C using  $Q_{10}$ .

Notes:

- <sup>a</sup> Rat hippocampal CA1 pyramidal cells (Magee and Johnston, 1995; Hoffman *et al.*, 1997).
- <sup>b</sup> Rat entorhinal cortex layer II cells (Magistretti and Alonso, 1999). The same subtypes can underlie both  $I_{Na}$  and  $I_{NaP}$  due to modulation by G-proteins; auxiliary subunits can slow down the inactivation of some  $Na_v$  subtypes (Köhling, 2002).
- <sup>c</sup> Activation kinetics from rat CA1 cells in vitro (Jaffe *et al.*, 1994; Magee and Johnston, 1995). Inactivation kinetics from cultured chick dorsal root ganglion neurons (Fox *et al.*, 1987). Calcium-dependent inactivation can also be modelled (Gillies and Willshaw, 2006).
- <sup>d</sup> Rat neocortical pyramidal neurons (Brown *et al.*, 1993).
- <sup>e</sup> CA1 cells in rat hippocampus (Jaffe *et al.*, 1994; Magee and Johnston, 1995).
- <sup>f</sup> CA1 cells in rat hippocampus (Jaffe *et al.*, 1994; Magee and Johnston, 1995).
- <sup>g</sup> Gillies and Willshaw (2006), based on rat subthalamic nucleus (Wigmore and Lacey, 2000).
- <sup>h</sup> Guinea pig hippocampal CA1 cells (Sah *et al.*, 1988).
- <sup>i</sup> Rat hippocampal CA1 pyramidal cells; underlying channel protein probably  $K_v4.2$  (Hoffman *et al.*, 1997). Expression of different auxiliary subunits can convert DR currents into A-type currents (Heinemann *et al.*, 1996).
- <sup>j</sup> Guinea pig hippocampal CA1 pyramidal cells (Halliwell and Adams, 1982); modelled by Borg-Graham (1989). See Jentsch (2000) for identification of channel proteins.
- <sup>k</sup> Rat hippocampal CA1 pyramidal neurons (Storm, 1988); modelled by Borg-Graham (1999). See Metz *et al.* (2007) for identification of channel proteins.
- <sup>l</sup> Guinea pig thalamic relay cells in vitro;  $E_h = -43$  mV (Huguenard and McCormick, 1992).
- <sup>m</sup> Rat muscle (Moczydlowski and Latorre, 1983) and guinea pig hippocampal CA3 cells (Brown and Griffith, 1983). Inactivation sometimes modelled (Borg-Graham, 1999; Section 5.6).
- <sup>n</sup> Rat  $K_{Ca}2.2$  expressed in *Xenopus* oocytes (Hirschberg *et al.*, 1998). Model in Section 5.6.
- <sup>o</sup> Borg-Graham (1999) based on various data. Channel proteins underlying  $I_{sAHP}$  are unknown (Section 5.6).

2004). In many instances, one channel gene can give rise to many different channel proteins, due to alternate splicing of RNA and RNA editing (Hille, 2001). Also, these channel types refer only to the sequences of the principal subunits; as covered in Section 5.1, the coexpression of auxiliary subunits modifies the behaviour of the principal subunits, sometimes dramatically. There is even more channel diversity than the plethora of gene sequences suggests.

## 5.3 Experimental techniques

### 5.3.1 Single channel recordings

A major advance in our understanding of channels came with the development of the **patch clamp technique** (Neher and Sakmann, 1976), where a fine glass pipette is pressed against the side of a cell (Figure 5.5). The rim of the pipette forms a high-resistance seal around a small patch of the membrane, so that most of the current flowing through the patch of membrane has to flow through the pipette. Seals with resistances of the order of gigohms can be made, and have been dubbed **gigaseals** (Hamill *et al.*, 1981). This allows for much less noisy recordings and makes it possible to record from very small patches of membrane.

In the low-noise recordings from some patches, the current can be observed to switch back and forth between zero and up to a few picoamperes (Figure 5.6). This is interpreted as being caused by the opening and closing of a single channel. The times of opening and closing are apparently random, though order can be seen in the statistics extracted from the recordings. For example, repeating the same voltage clamp experiment a number of times leads to an **ensemble** of recordings, which can be aligned in time, and then averaged (Figure 5.6). This average reflects the probability of a channel being open at any time. The **macroscopic** currents (for example, those recorded by Hodgkin and Huxley), appear smooth as they are an ensemble average over a large population of **microscopic** currents due to stochastic channel events.

### 5.3.2 Channel isolation by blockers

Hodgkin and Huxley (1952d) succeeded in isolating three currents with distinct kinetics (the sodium, potassium delayed rectifier and leak currents). Since then, many more currents with distinct kinetics have been isolated. The process was expedited by the discovery of **channel blockers**, pharmacological compounds which prevent certain types of current flowing. First to be discovered was tetrodotoxin (TTX), which is isolated from the Japanese puffer fish and blocks  $\text{Na}^+$  channels involved in generating action potentials (Narahashi *et al.*, 1964). Likewise tetraethylammonium (TEA) was found to block some types of  $\text{K}^+$  channel (Hagiwara and Saito, 1959). Subsequently, many more compounds affecting ion channel behaviour have been discovered (Hille, 2001). Appendix A provides links to the comprehensive lists of blockers for various channel subtypes that can be found online in the *IUPHAR Compendium of Voltage-gated Ion Channels* (Catterall and Gutman, 2005) and the *Guide to Receptors and Channels* (Alexander *et al.*, 2008).

Neher and Sakmann received a Nobel prize for their work in 1991. The methods of forming high-resistance seals between the glass pipette and the membrane proved fundamental to resolving single channel currents from background noise.

The puffer fish is a delicacy in Japan. Sushi chefs are specially trained to prepare the fish so as to remove the organs which contain most of the toxin.



**Fig. 5.6** Single channel recordings of two types of voltage-gated calcium channel in guinea pig ventricular cells (Nilius *et al.*, 1985), with 110 mM  $\text{Ba}^{2+}$  in the pipette. **(a)** The single channel currents seen on seven occasions in response to a voltage step to a test potential of 10 mV (top). The bottom trace shows the average of 294 such responses. It resembles the Hodgkin–Huxley sodium current. This channel, named **L-type** for its long-lasting current by Nilius *et al.* (1985), belongs to the  $\text{Ca}_v1$  family of mammalian calcium channels. **(b)** Single channel and ensemble responses to a voltage step to the lower potential of  $-20$  mV. The ensemble-averaged current inactivates more quickly. This channel, named **T-type** because of its transient nature by Nilius *et al.* (1985), belongs to the  $\text{Ca}_v3$  family of mammalian channels. Reprinted by permission from Macmillan Publishers Ltd: *Nature* 316, 443–446, © 1985.

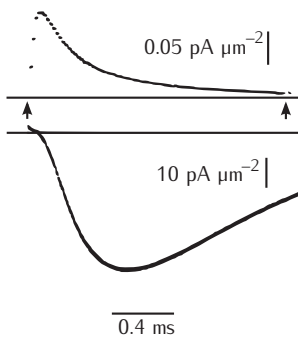
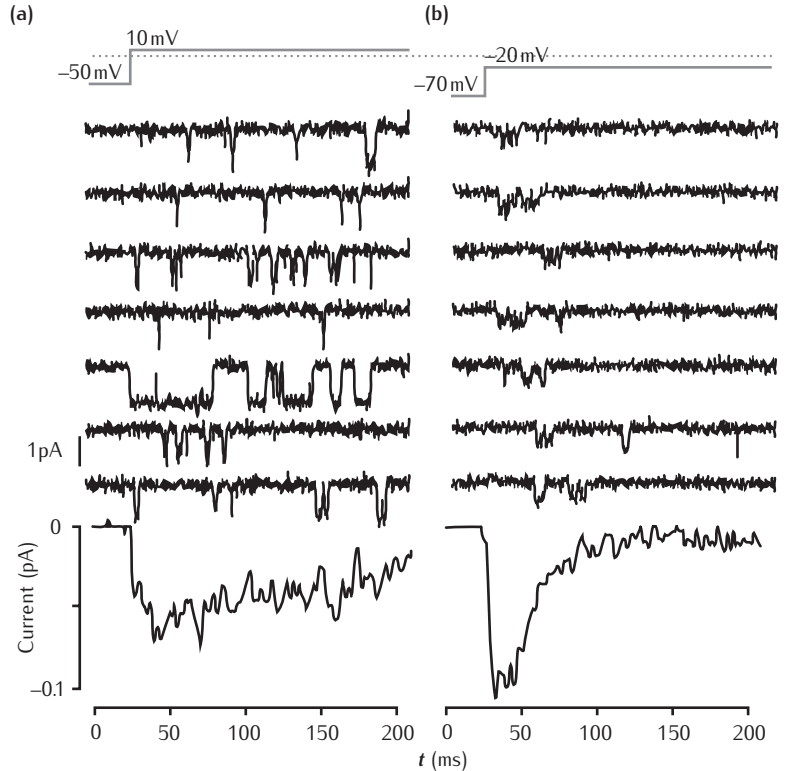


**Fig. 5.7** Gating current (above) and ionic current (below) in squid giant axon sodium channels, measured by Armstrong and Bezanilla (1973). Reprinted by permission from Macmillan Publishers Ltd: *Nature* 242, 459–461, © 1973.

### 5.3.3 Channel isolation by mRNA transfection

Since the 1980s the molecular biological method of **heterologous expression** has been used to isolate channels. Heterologous expression occurs when the cloned DNA (cDNA) or messenger RNA (mRNA) of a protein is expressed in a cell which does not normally express that protein (Hille, 2001). Sumikawa *et al.* (1981) were the first to apply the method to ion channels, by transfecting oocytes of the amphibian *Xenopus laevis* with the mRNA of acetylcholine receptors and demonstrating the presence of acetylcholine channels in the oocyte by the binding of bungarotoxin. Subsequent voltage clamp experiments demonstrated the expression of functional acetylcholine channel proteins in the membrane (Mishina *et al.*, 1984). This approach has been extended to mammalian cell lines such as CHO (Chinese hamster ovary), HEK (human embryonic kidney) and COS (monkey kidney) (Hille, 2001). Thus channel properties can be explored in isolation from the original cell.

While heterologous expression gives a clean preparation, there are also potential pitfalls, as the function of ion channels can be modulated significantly by a host of factors that might not be present in the cell line, such as intracellular ligands or auxiliary subunits (Hille, 2001).

### 5.3.4 Gating current

The movement of the gating charges as the channel protein changes conformation leads to an electric current called the **gating current**, often referred

to as  $I_g$  (Hille, 2001). Gating currents tend to be much smaller than the ionic currents flowing through the membrane. In order to measure gating current, the ionic current is reduced, either by replacing permeant ions with impermeant ones or by using channel blockers, though the channel blocker itself may interfere with the gating mechanism. Other methods have to be employed to eliminate leak and capacitive currents. Figure 5.7 shows recordings by Armstrong and Bezanilla (1973) of the gating current and the sodium ionic current in response to a voltage step. The gating current is outward since the positively charged residues on the membrane protein are moving outwards. It also peaks before the ionic current peaks.

Gating currents are a useful tool for the development of kinetic models of channel activation. The measurement of gating current confirmed the idea of charged gating particles predicted by the HH model. However, gating current measurements in squid giant axon have shown that the HH model is not correct at the finer level of detail (Section 5.5.3).

## 5.4 Modelling ensembles of voltage-gated ion channels

### 5.4.1 Gating particle models

Before the detailed structure and function of ion channels outlined in Section 5.1 was known, electrophysiological experiments indicated the existence of different types of channel. Various blocking and subtraction protocols led to the isolation of specific currents which displayed particular characteristics.

#### The A-type current

To take one example, the potassium **A-type** current, often denoted  $I_A$ , has distinct kinetics from the potassium delayed rectifier current, denoted  $I_{DR}$  or  $I_K$  or  $I_{K,DR}$ , originally discovered by Hodgkin and Huxley. Connor and Stevens (1971a, c) isolated the current by using ion substitution and by the differences in current flow during different voltage clamp protocols in the somata of cells of marine gastropods. The A-type current has also been characterised in mammalian hippocampal CA1 and CA3 pyramidal cells using TTX to block sodium channels (Figure 5.8).

In contrast to the delayed rectifier current, the A-type current is inactivating, and has a lower activation threshold. It has been modelled using independent gating particles by a number of authors (Connor and Stevens, 1971b; Connor *et al.*, 1977; Hoffman *et al.*, 1997; Poirazi *et al.*, 2003). In the model of Connor *et al.* (1977), the A-type current in the crustacean *Cancer magister* (Box 5.2) depends on three independent activating gating particles and one inactivating particle. In contrast, Connor and Stevens (1971b) found that raising the activating gating variable to the fourth power rather than the third power gave the best fit to the A-type current they recorded from the somata of marine gastropods.

The significance of the A-type current is illustrated clearly in simulations of two neurons, one containing sodium and potassium conductances

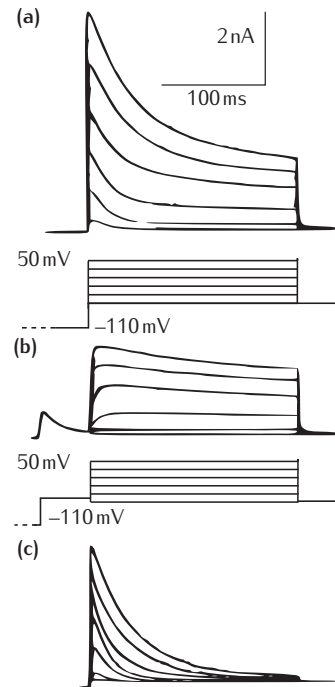


**Fig. 5.8** Recordings of two types of potassium channel revealed by different voltage clamp protocols in hippocampal CA1 cells. **(a)** Family of voltage clamp current recordings from CA1 cells subjected to the voltage step protocol shown underneath. **(b)** The voltage was clamped as in **(a)**, except that there was a delay of 50 ms before the step to the depolarising voltage. **(c)** Subtraction of trace in **(b)** from trace in **(a)** reveals a transient outward current known as the A-type current. Adapted from Klee *et al.* (1995), with permission from The American Physiological Society.